CrossMark

ORIGINAL ARTICLE

Transcranial LED therapy on amyloid-β toxin 25–35 in the hippocampal region of rats

Camila da Luz Eltchechem[1] · Afonso Shiguemi Inoue Salgado[2] ·
Renato Amaro Zângaro[3] · Mário César da Silva Pereira[1] · Ivo Ilvan Kerppers[1] ·
Luis Augusto da Silva[4] · Rodolfo Borges Parreira[2]

Abstract Excessive Aβ deposition in the brain is associated with the formation of senile plaques, and their diffuse distribution is related to Alzheimer's disease. Thirty rats (EG) were irradiated with light-emitting diode (photobiomodulation (PBM)) in the frontal region of the skull after being inoculated with the Aβ toxin in the hippocampus; 30 rats were used as the control group (CG). The analysis was conducted at 7, 14, and 21 days after irradiation. We observed a decreased in Aβ deposits in treated animals compared with animals in the CG. The behavioral and motor assessment revealed that the EG group covered a larger ground distance and explored the open field than the CG group on days 14 and 21 ($p < 0.05$). The EG group was statistically significant in the spatial memory test compared to the CG group on day 14. The use of PBM significantly reduced the presence of Aβ plaques and improved spatial memory and behavioral and motor skills in treated animals on day 21.

Introduction

Alzheimer's disease (AD) is a progressive neurodegenerative disorder clinically characterized by cognitive and memory dysfunction accompanied by classical hallmark pathologies such as intraneuronal neurofibrillary tangles (NFTs) and extracellular amyloid plaques [1–3].

The excessive deposition of the amyloid-β (Aβ) protein in the brain with the formation of senile plaques and their diffuse distribution in the cerebral cortex results in the progressive loss of synapses in extensive areas providing the earliest clinical signs of AD: short-term memory loss [3]. The role of neuroinflammation and oxidative stress in AD has already been established [4].

✉ Ivo Ilvan Kerppers
ikerppers@gmail.com

Camila da Luz Eltchechem
caah_s2@hotmail.com

Renato Amaro Zângaro
razangaro@gmail.com

Mário César da Silva Pereira
mcpereira@unicentro.br

Luis Augusto da Silva
lasilva7@hotmail.com

Rodolfo Borges Parreira
dolfo23@yahoo.com

1   Laboratory of Neuroanatomy and Neurophysiology for the Physiotherapy, Universidade Estadual do Centro-Oeste, Rua Simeão Camargo Varela de Sá, 03, Guarapuava, Paraná, Brazil 85040-080

2   School of Postural and Manual Therapy, Salgado Institute of Integral Health, Londrina, Paraná, Brazil 86015-300

3   Center for Innovation, Technology and Education (CITÉ), São José dos Campos, São Paulo, Brazil 12245-650

4   Laboratory of Biomedical Science for the Pharmacy, Universidade Estadual do Centro-Oeste, Guarapuava, Paraná, Brazil 85040-080

🍬 Springer

They cause an accumulation of plaques because Aβ peptide active astrocytes and microglia participate in the production of toxins and inflammatory cytotoxins, contributing to the neurodegenerative process [5–7], and thus creating a vicious circle. The Aβ peptide is produced by the cleavage of the protein called amyloid precursor protein.

Once formed and released into the extracellular environment, Aβ has two destinations: it can remain in its monomeric form or initiates the process of polymerization, which will form oligomers and/or fibrils [8]. In cases of AD, the presence of anomalous proteins, particularly the Aβ peptide, can trigger oxidative stress through the formation of reactive species of oxygen and nitrogen (ROS), which in turn, are significant in the occurrence of mitochondrial injuries [4].

The mitochondrial collapse that follows seems to be caused by the direct toxic action of the Aβ peptide, which leads to synaptic loss, cellular death, oxidative stress, and inflammation; these processes have been implicated in several neurodegenerative diseases, including AD [4, 9]. Low-level laser/light-emitting diode (LED) therapy (LLLT) (<200 mW) or even noncoherent LEDs in the red or near-infrared (NIR) wavelength range are commonly known as photobiomodulation (PBM) [10].

Lasers (coherent radiation) and LEDs (noncoherent radiation) produce beneficial cellular effects in controlled trials [10]. During the LLLT, the absorption of red or NIR photons by the cytochrome c oxidase in the mitochondrial respiratory chain cause an increase in cellular respiration at appropriate energy and power densities [11].

The effects include an increase in mitochondrial respiration, ATP synthesis [12–14], and nerve cell proliferation [15], among others. Through the analysis of increased cytochrome oxidase, Rojas et al. [16] reported that PBM induces brain metabolic and antioxidant effects. In another study, these authors reported an increase in memory retention and oxygen consumption as the result of cytochrome oxidase stimulation in the frontal cortex of rats [17].

Significant results were seen when transcranial PBM was applied in neurodegenerative diseases, such as in Parkinson's and Alzheimer's diseases that were experimentally induced in rats [18–20].

At this time, few studies have been conducted to evaluate the use of LED therapy and its effects on senile plaques and behavior state related to the AD model in rats following a treatment protocol with PBM. This study is based on previous studies regarding the physiological effects of LED over neurological tissue and cell structures in neurological diseases. Our hypothesis is that this treatment will improve impaired behavioral states in rats with AD through the photobiological action of the treatment, diminishing the presence of senile plaques.

The main objective of the present study was to evaluate the effect of PBM (LED 627 nm) treatment on the presence of senile plaques in rats with AD induced by the administration of Aβ$_{25–35}$ toxin in the hippocampal region and on their spatial memory and behavioral state.

Methods

Sample

The sample was composed of 60 male Wistar rats (Rattus Norvegicus) weighing between 200 and 250 g. They were placed in acrylic cages in pairs and kept in a light/dark cycle of 12 h with water and food ad libitum. The present study was approved by the Animal Use Ethics Committee of the Midwest State University (Unicentro) under protocol number 045/2013. All procedures were conducted in accordance with the CEUA.

Directive for experiments including animals

Animals were divided into two groups, treated and nontreated; they were subsequently subdivided into six groups of ten animals in each group as follows: nontreated for 7 days and euthanasia on day 8, nontreated for 14 days and euthanasia on day 15, nontreated for 21 days and euthanasia on day 22, treated for 7 days and euthanasia on day 8, treated for 14 days and euthanasia on day 15, and treated for 21 days and euthanasia on day 22.

Surgical procedure for the Aβ$_{25–35}$ inoculation

The Aβ$_{25–35}$ 1 MG protein was acquired from the Sigma-Aldrich and used dissolved in 0.1 μl of DMSO and 0.9 μl of distilled water; this solution was incubated for 72 h at 4 °C. Animals (n = 60) were anesthetized intra-abdominally with a solution in the proportion of 80 mg/kg of hydrochloride ketamine (Ketamine, 10 ml bottle) to 15 mg/kg of hydrochloride xylazine (Dopaser, 10 ml bottle) and taken to a stereotaxic apparatus (David Kopf, EUA) where their heads were fixated by the temporal bone and upper incisors. Cannulas made with 30 × 09 needles (5 mm long) were implanted in the hippocampal region and directed to the hippocampus CA1 area according to the stereotaxic coordinates in the atlas by Paxinos and Watson [21]. The following stereotaxic coordinates were used: AP = −3.12 mm, ML = ± 1.8 mm, and DV = 2.8 mm using bregma as a reference and lambdoid and bregmatic sutures on the same horizontal plane. After the implants were placed, the cannulas were fixated in the calvaria using a self-curing acrylic prosthesis. A stainless steel wire was inserted into the cannula to prevent occlusion. A screw was placed in the anterior section of the skullcap to fixate the wire. The animals were allowed to rest for 5 days before being anesthetized again and submitted to the stereotactic process for the

$A\beta_{25-35}$ inoculation. Using a Hamilton syringe, 2 μl of the $A\beta_{25-35}$ (Sigma-Aldrich) peptide was inoculated in the CA1 region of the hippocampus as described in Freir and Herron [22]. The peptide solution was injected at 0.1 μl per minute (with a total time of 20 min) to prevent backflow and allow the toxin to be absorbed into the brain parenchyma.

Study characterization

Animals rested for 21 days after the intracerebral injection; one animal from each group was randomly selected to be euthanized for the verification of presence of senile plaques in the brain; if senile plaques were present, the study proceeded (Fig. 1).

Protocol assessments

Behavioral and locomotor measurement

The open field test [23] provides simultaneous measurements of locomotion, exploration, and anxiety. To conduct the test, animals were individually placed in the center of an arena and exposed to the open field for a period of 5 min and their behaviors were filmed. The etiological analysis of their behavior assessed the following: frequency and duration of walking, standing and grooming, and the number of fecal boli. Walking was measured by the number of rectangles covered using all four paws. Standing was considered when the animals supported themselves solely on the hind paws. Grooming was considered as movements of the front paws along the head or body. Fecal boli were counted after the animal was removed from the arena. The arena floor was cleaned with alcohol and extensively dried, and air was allowed circulating between each animal.

Spatial memory assessment

The Morris water maze [24] was used to assess spatial memory. This test was firstly described 20 years ago to investigate spatial learning and memory in rats. The Morris water maze consisted of a circular tank (90 cm in diameter, 50 cm in height) filled with water to a depth of 29 cm and maintained at 24 ± 1 °C. Four points are established to the north, south, east, and west (N, S, E, W) edges of the pool. In the center of one of the four quadrants, based on these cardinal points, there is a platform, invisible to the rat, placed at approximately 2 cm below the water level. This acrylic platform is transparent with an area of 11×14 cm on which the animal can support itself and escape from the water. The walls of the pool contain visual hints composed of geometric designs and figures that serve as reference points for the animal.

Protocol for irradiation

The Superbrightled model RL5-R12008 PBM transducer was used at 627-nm emission. The optical power of the device was previously measured by the ThorLabs optical wattmeter model PM100D, which was set at 70 mW and 627 nm [25]. The PBM system contains seven LEDs with an encapsulated LED diameter of 5 mm. The LEDs were geometrically arranged circumferentially with an angle of 15° in their order of irradiation, forming one dot that focuses the light on one single location in order to achieve useful irradiation intensity levels for the clinical application of phototherapy. Inside the device, a spacer projected an irradiation area of 1 cm^2 on the sample; the encapsulated LEDs were placed at 1 cm from the scalp. The application method was based on time. The PBM system was stationary positioned in skin contact at the frontal region in the rat's head; the irradiation was applied once a day for 100 s, at the irradiation dose of 7 J/cm^2 with potency of 70 mW for 21 days.

Histological analysis

Animals were euthanized in a CO_2 chamber, and death was confirmed visually. The brain was removed, sectioned near the cannula channel, placed in 10% formalin, sent to the pathology laboratory, and placed in paraffin. Three 2-μm sections with an interspace of 10 μm were cut and stained with hematoxylin and eosin (HE) and with other dyes for the immunohistochemical analysis.

Statistical analysis

The data were analyzed with the SPSS 20.0 software. One-way ANOVA and the Tukey's post hoc test were used in the parametric data, and the Mann–Whitney U test was used in the nonparametric data. Differences were considered statistically significant at $p \leq 0.05$.

Results

Histological analysis

The histological analysis showed that at 7, 14, and 21 days after the PBM treatment, all irradiated groups showed a significant reduction in the amount of Aβ as indicated by blue arrows compared to the nontreated group at 21 days (Fig. 2). Figure 2a, b displays the limited presence of Aβ plaques in both groups after 7 days. Morphological alterations in the hippocampal region were evident in the treated group. However, there was a large quantity of astrocytes around the injured region in the nontreated group (severe level) while the presence of these cells was lower in the treated group (intense
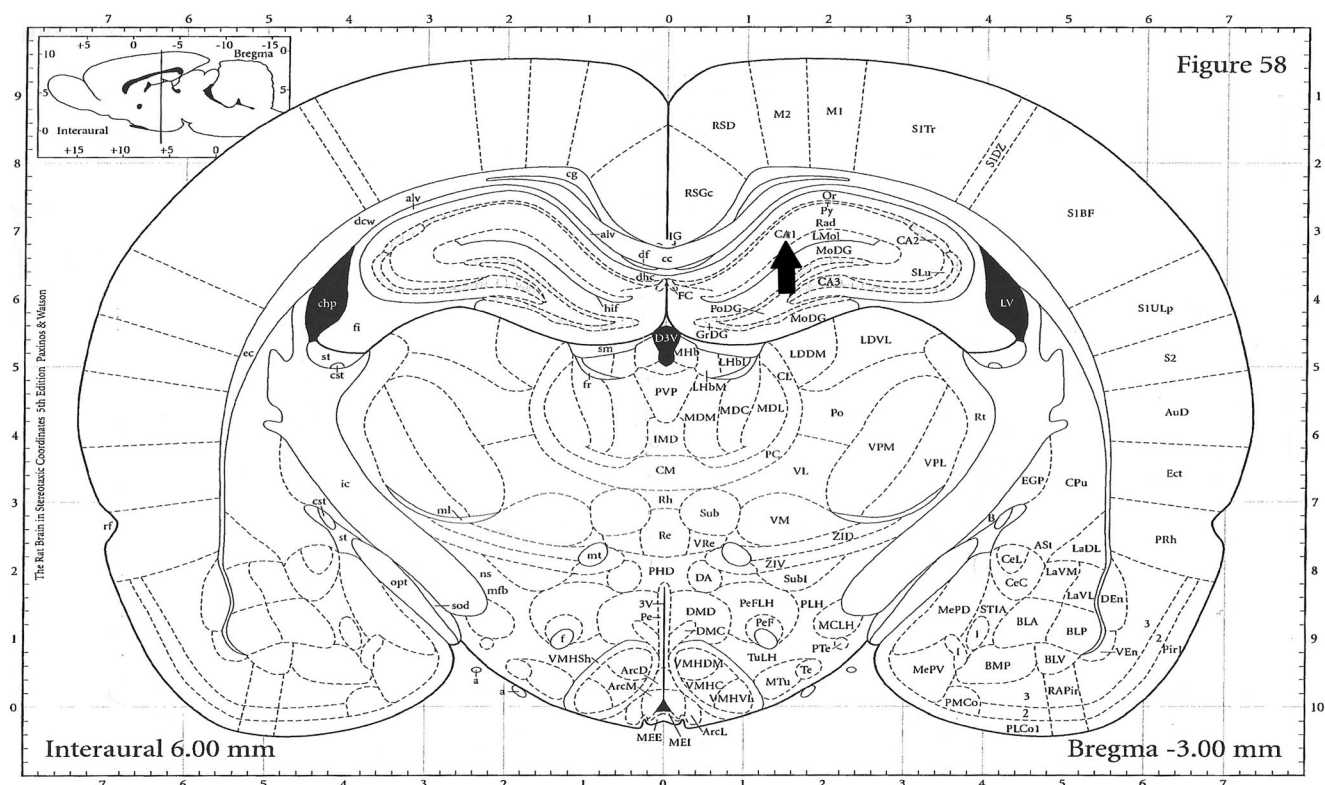
Fig. 1 The *circle* demarcates the location where the induction of the process for the deposition of beta amyloid toxin occurred

level). On day 14 (Fig. 2c, d, as indicated by the yellow arrow in A) in the nontreated group, an intense presence of senile plaques in the hippocampus was observed distributed throughout the CA1 anterior region, intense presence of astrocytes throughout the tissue, and a morphological increase of the hippocampus. An intense presence of senile plaques was observed in the treated group; however, it was distributed throughout the hippocampus with a moderate presence of astrocytes. On day 21, extensive tissue necrosis with severe deposition of Aβ plaques, morphological alterations in the hippocampus, intense edema and severe levels of immune glial cells were observed in the nontreated group. In the treated group, a moderate level of senile plaques and a mild presence of astrocytes was observed throughout the hippocampal region (Fig. 2e, f).

The immunohistochemical analysis shows positive results for markers for the presence of the beta amyloid protein was lower in the treated group than in the untreated group (Fig. 2a–f).

Behavioral and locomotor measurement

Figure 3 shows the presence of plaques on days 7, 14, and 21 between groups. The quantification of plaques through antibody immunohistochemistry showed that the amount of senile plaques in the hippocampal region increased over time from the Aβ toxin inoculation in the nontreated

group compared to treated group on day 14. On day 21, the nontreated group showed greater amount of senile plaques than on days 7 and 14 ($p < 0.001$). The statistical analysis showed a significant difference ($p < 0.001$) when compared with the treated group on day 21, when we could observe that senile plaques did not progress in relation to day 14 in the treated group.

Figure 4 shows the distance traveled by the rats in the open field test. After 7 days of irradiation, the animals in the treated group covered a mean distance of 1250 ± 154.3 cm whereas those in the nontreated group covered a mean distance of 380.8 ± 142.8 cm; however, these results were not statistically significant ($p > 0.05$). The distances covered by animals in the treated and untreated groups were 1428 ± 16.79 and 476.2 ± 16.79 cm ($p = 0.028$) and 734.6 ± 59.5 and 1975 ± 276.8 cm ($p = 0.028$) after 14 and 21 days, respectively.

With regards to the Morris water maze test (Fig. 4), a statistically significant difference was observed between the groups after 14 days of PBM irradiation; the animals in the treated group required a mean time of 1.748 ± 0.56 s to find the center of the maze whereas those in the nontreated group required 4.533 ± 0.12 s ($p = 0.028$). No statistical differences ($p > 0.05$) were observed between groups on day 7 and 21. On day 7, the animals in the treated and nontreated groups required mean times of 2.833 ± 0.34 and 3.645 ± 0.98 ($p =$

Fig. 2 Histological analysis after the PBM treatment
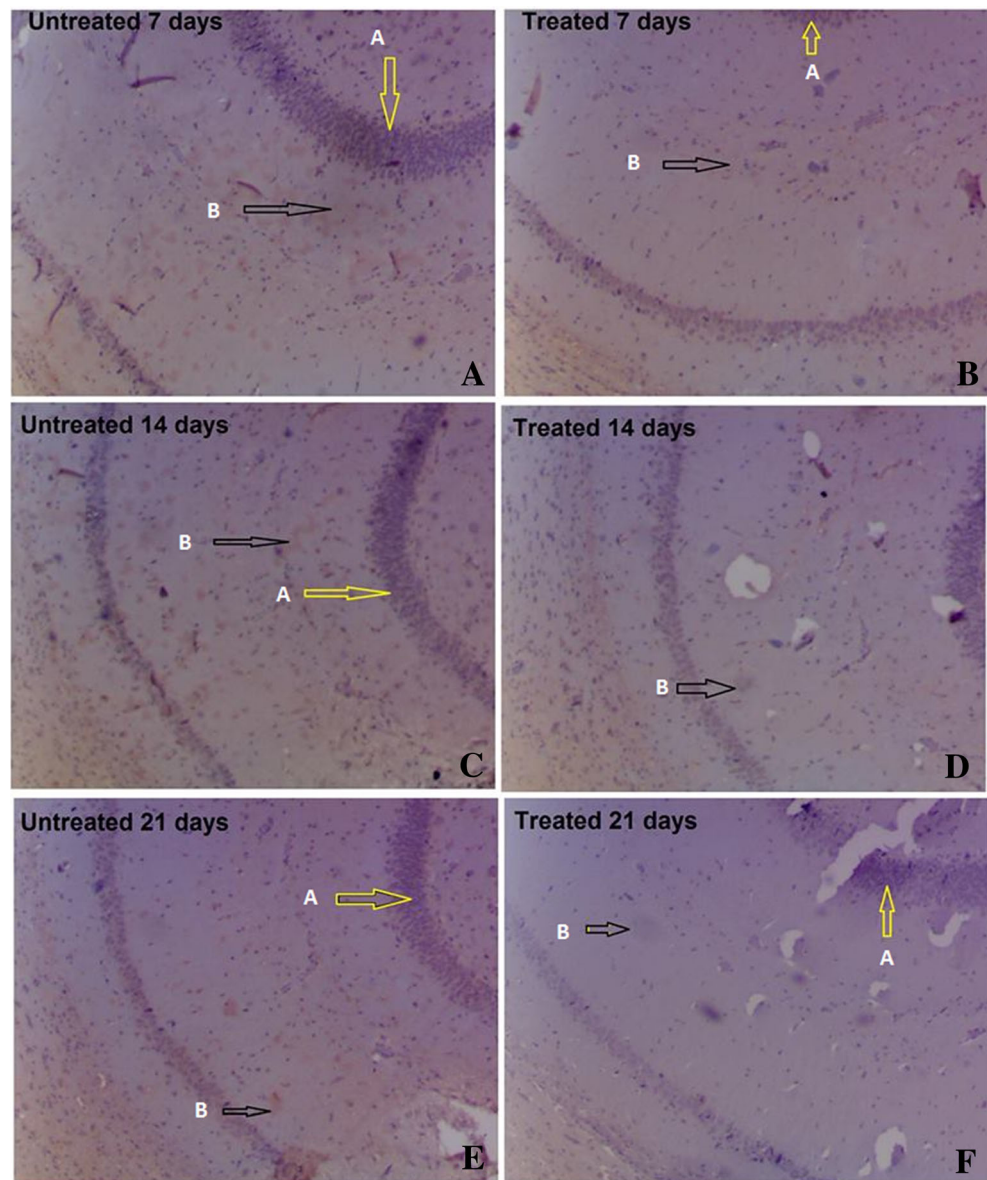
0.23), respectively. The mean speed was 2.475 ± 0.78 and 4.72 ± 1.02 on day 21 in the treated and non-treated groups, respectively.

Discussion

Few studies have demonstrated the action of phototherapy with positive effects on neurological conditions such as AD, Parkinson's disease, and dementia. The results of the present study confirm the benefits of the PBM treatment in the Alzheimer's disease model using the inoculation of $A\beta_{25-35}$ in rats. Here, we observe a decrease in Aβ toxin deposits in the hippocampal

region with improved performance in behavioral and motor tests.

Effects of PBM on senile plaques

Our study evaluated the deposition of Aβ between 7 and 21 days in rats. The nontreated group shows the greatest amounts of this protein, particularly on day 21. This finding demonstrates that the accumulation of Aβ in the hippocampal region leads to significant immunological alterations such as increased levels of Aβ toxin, astrocytes, and glial cells in comparisons between treated and nontreated groups. The PBM treatment promotes positive results in the inflammatory process decreasing the levels of βA (Fig. 2c–f). The

Mean and Standard Deviation for Toxin Beta amyloid
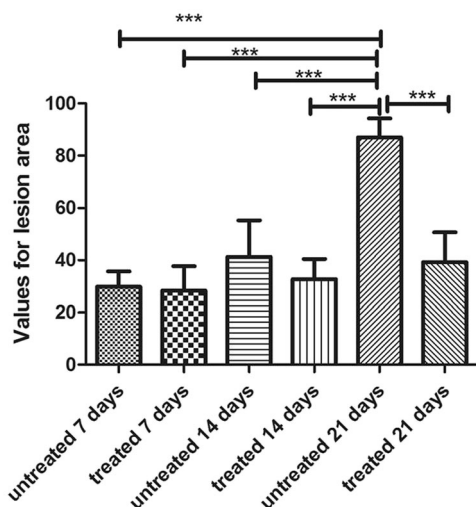
Fig. 3 Mean and standard deviation for toxin beta amyloid

accumulation of Aβ in the brain is one of the main pathological processes in AD patients. The formation of these deposits initiates a series of cellular events that can elicit an immune response involving cells such as those in the microglia and astrocytes, which secrete pro-inflammatory by-products such as cytokines and prostaglandins [4–8] and play an important role in AD [6]. This process was observed in the histological analysis in our study (Figs. 2 and 3) through an intense presence of astrocytes in the nontreated group, which resulted in a severe deposition of amyloid plaques. Hashmi et al. [26] reported that the PBM treatment assists in preventing neurodegenerative diseases due to the activation of transcription factors that lead to the expression of many protective factors such as antioxidants and antiapoptotic factors. Hanczyc et al. [27] explain these effects by showing that amyloid fibrils, which includes Aβ, have great ability to absorb photons due the presence of chromophores in the molecular structure of their fibrils, thus confirming the phototherapeutic effects of the PBM treatment.

According to Yang et al. [28], irradiation with LED induces nerve regeneration after trauma and reduces the inflammatory

process, which supports the observation of extensive tissue necrosis in the intense edema and severe levels of glial cells (Fig. 2e, f) on day 21 in our study. The same authors used LED 632.8 nm and reported a reduction in the formation of Aβ, which inhibited the production of ROS and the presence of astrocytes. Bortoletto et al. [29] and Giuliani et al. [30] reported that the use of low-level laser therapy increased ATP synthesis and that the modulation of oxidative stress occurs in PC12 cells under infrared light.

Sommer et al. [20] applied LED 670 nm in cultured cells and confirmed a reduction of Aβ. The same authors proposed the LED application as a treatment for AD.

According to Yang et al. [7], senile plaques are surrounded by activated microglia and astrocytes, which secrete pro-inflammatory factors in the area such as cytokines and prostaglandins. Sofroniew and Vinters [31] report that astrocytes (glial cells) play an important role in the organization and maintenance of the brain interacting with neurons that are involved in the secretion of neurotransmitters and modulation of oxidative stress. An interesting result in our study was the presence of increased agglomeration in the dentate gyrus (Fig. 2; B—treated group on day 21). This structure is also responsible for neurogenesis where any of these cells, after formation, will functionally integrate around the brain [32]. Costa et al. [33] showed in their study that the dentate gyrus would be responsible for implementing spatial and temporal tasks in rats. Therefore, we could infer that the PBM treatment stimulates the dentate gyrus to produce cortical neurons and thereby improve cognitive performance.

Effects of PBM on spatial memory and behavioral state

The hippocampus and its subregions, for example, the dentate gyrus, are responsible areas mediating the recognition of configurations, spatial and temporal behavior, and episodic memory [34–36]. It also displays particular importance in memory and learning processes [37]. In AD, Counts et al. [36] reported that prior to the onset of disease, a premature disruption occurs in the CA1 area gene affecting the cascade of molecular events

Fig. 4 Distance traveled by the rats in the open field test

755
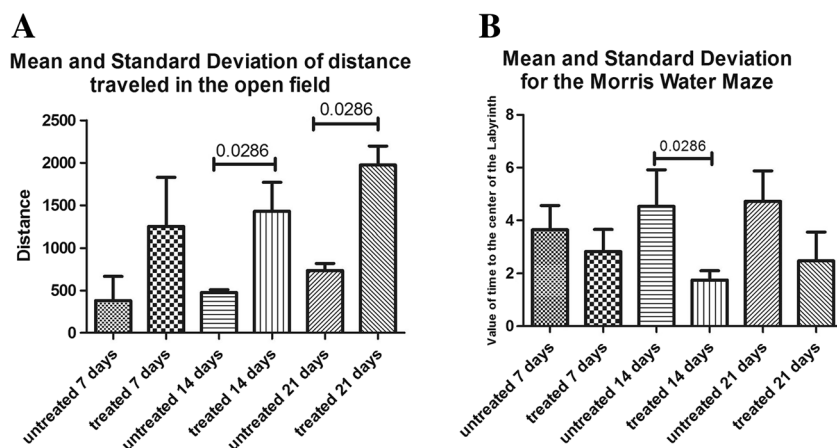
that will trigger AD, which leads to a synaptic failure causing cognitive impairment. In the present study, both treated and untreated groups did not differ in the distance traveled in the open field test and Morris water maze test (Fig. 4) on day 7 post-Aβ inoculation, demonstrating that a lesion in this area could harm or affect motor and behavioral tasks.

Some studies have shown that lesions in the hippocampus and dentate gyrus affect the process of recognition and performance in spatial and temporal tasks. Bueno et al. [37] showed that rats with an experimentally caused injury in the dentate gyrus were able to acquire tasks; however, their memory acquisition process becomes slower and they lose spatial and temporal discrimination acuity. Eichenbaum et al. [38] demonstrated that rats, even with hippocampal lesions, were skilled in the Morris water maze task. Our results in the Morris water maze show that there was no difference between groups in the late stage of AD; however, the PBM-treated group showed better performance than the untreated group.

Our study is the first to demonstrate the effects of PBM in AD models on behavioral and locomotor tasks. Michalikova et al. [39] report that rats exposed to infrared radiation show an improvement in cognitive and behavioral aspects.

Our study indicates the beneficial effect of PBM treatment on behavioral tasks in the early stages of AD by demonstrating the improvement in motor and behavioral performance in treated animals compared to nontreated ones.

Conclusion

The use of PBM in rats with AD showed a significant reduction in senile plaques after 21 days of treatment in the treated group compared to the nontreated group. Moreover, the results of the evaluation of behavioral motor state were satisfactory. The early diagnosis of AD associated with the proposed use of PBM, which is a low-cost and noninvasive procedure and with absolute unknown contraindications, could lead to the achievement of relevant results that would improve the quality of life of people affected by this disease. Further investigation using a population of patients with AD is required.

References

1. Zheng H, Koo EH (2011) Biology and pathophysiology of the amyloid precursor protein. Mol Neurodegener 6:27
2. Lee VM, Goedert M, Trojanowski JQ (2001) Neurodegenerative tauopathies. Annu Rev Neurosci 24:1121–1159
3. Hippius H, Neundorfer G (2003) The discovery of Alzheimer's disease. Dialogues Clin Neurosci 5:101–108
4. Fisher R, Maier O (2015) Interrelation of oxidative stress and inflammation in neurodegenerative disease: role of TNF. Oxidative Med Cell Longev 2015:610813
5. McGeer PL, McGeer EG (2002) Local neuroinflammation and the progression of Alzheimer's disease. J Neurovirol 8:529–538
6. Perry VH, Nicoll JAR, Holmes C (2010) Microglia in neurodegenerative disease. Nat Rev Neurol 6:193–201
7. Yang H, Feng G, Liang Z, Vitale A, Jiao XY, Ju G, You SW (2012) In vitro beneficial activation of microglial cells by mechanically-injured astrocytes enhances the synthesis and secretion of BDNF through p38MAPK. Neurochem Int 6:175–186
8. Haass C, Selkoe DJ (2007) Soluble protein oligomers in neurodegeneration: lessons from the Alzheimer's amyloid beta-peptide. Nat Rev Mol Cell Biol 8:101–112
9. Heneka MT, O'Banion MK (2007) Inflammatory processes in Alzheimer's disease. J Neuroimmunol 184:69–91
10. Desmet KD, Paz DA, Corry JJ, Eells JT, Wong-Riley MTT, Henry MM, Buchmann EV, Connelly MP et al (2006) Clinical and experimental applications of NIR-LED photobiomodulation. Photomed Laser Surg 24:121–128
11. Lane N (2006) Cell biology: power games. Nature 443:901–903
12. Yu W, Naim JO, McGowan M, Ippolito K, Lanzafame RJ (1997) Photomodulation of oxidative metabolism and electron chain enzymes in rat liver mitochondria. Photochem Photobiol 66:866–871
13. Mochizuki-Oda N, Kataoka Y, Cui Y, Yamada H, Heya M, Awazu K (2002) Effects of near-infra-red laser irradiation on adenosine triphosphate and adenosine diphosphate contents of rat brain tissue. Neurosci Lett 323:207–210
14. Oron U, Ilic S, De Taboada L, Streeter J (2007) Ga-As (808 nm) laser irradiation enhances ATP production in human neuronal cells in culture. Photomed Laser Surg 25:180–182
15. Oron A, Oron U, Chen J, Eilam A, Zhang C, Sadeh M, Lampl Y et al (2006) Low-level laser therapy applied transcranially to rats after induction of stroke significantly reduces long-term neurological deficits. Stroke 37:2620–2624
16. Rojas J, Lee J, John J, Gonzalez-Lima F (2008) Neuroprotective effects of nearinfrared light in an in vivo model of mitochondrial optic neuropathy. J Neurosci 28:13511–13521
17. Rojas JC, Bruchey AK, Gonzalez-Lima F (2012) Low-level light therapy improves cortical metabolic capacity and memory retention. J Alzheimers Dis 32:741–752
18. Liang HL, Whelan HT, Eells JT, Wong-Riley MTT (2008) Near-infrared light via light-emitting diode treatment is therapeutic against rotenone- and 1-methyl-4-phenylpyridinium ion-induced neurotoxicity. Neuroscience 153:963–974
19. Duan R, Zhu L, Liu TCY, Li Y, Liu J, Jiao J, Xu X, Yao L, Liu S (2003) Light emitting diode irradiation protect against the amyloid beta 25–35 induced apoptosis of PC12 cell in vitro. Lasers Surg Med 33:199–203
20. Sommer AP, Bieschke J, Friedrich RP, Zhu D, Wanker EE, Fecht HJ, Mereles D, Hunstein W (2012) 670 nm laser light and EGCG complementarily reduce amyloid-β aggregates in human neuroblastoma cells: basis for treatment of Alzheimer's disease? Photomed Laser Surg 30:54–60
21. Paxinos G, Watson C (1998) The rat brain in stereotaxic coordinates. Academic, San Diego

22. Freir DB, Herron CE (2003) Inhibition of L-type voltage dependent calcium channels causes impairment of long-term potentiation in the hippocampal CA1 region in vivo. Brain Res 967:27–36
23. Walsh RN, Cummins RA (1976) The open-field test: a critical review. Psychol Bull 83:482–504
24. D'Hooge R, De Deyn PP (2001) Applications of the Morris water maze in the study of learning and memory. Brain Res Rev 36:60–90
25. Barbosa C, Teles C, Moreira L, Damião AJ, de Lima C (2012) A novel opto-mechanical system constituted by LEDs to employment in photobiostimulation: clinical application in optical therapy. Spectroscopy 27:9–18
26. Hashmi JT, Huang YY, Osmani BZ, Sharma SK, Naeser MA, Hamblin MR (2010) Role of low-level laser therapy in neurorehabilitation. PM R 2:S292–305
27. Hanczyc P, Samoc M, Norden B (2013) Multiphoton absorption in amyloid protein fibres. Nat Photonics 7:969–972
28. Yang Z, Zhang Y, Yang Y, Sun L, Han D, Li H, Wang C (2010) Pharmacological and toxicological target organelles and safe use of single-walled carbon nanotubes as drug carriers in treating Alzheimer disease. Nanomedicine 6:427–441
29. Bortoletto R, Silva NS, Zângaro RA, Pacheco MTT, Da Matta RA, Pacheco-Soares C (2004) Mitochondrial membrane potential after low-power laser irradiation. Lasers Med Sci 18:204–206
30. Giuliani A, Lorenzini L, Gallamini M, Massella A, Giardino L, Calzà L (2009) Low infra red laser light irradiation on cultured neural cells: effects on mitochondria and cell viability after oxidative stress. BMC Complement Altern Med 9:8
31. Sofroniew MV, Vinters HV (2010) Astrocytes: biology and pathology. Acta Neuropathol 119:7–35
32. Aimone JB, Deng W, Gage FH (2011) Resolving new memories: a critical look at the dentate gyrus, adult neurogenesis, and pattern separation. Neuron 70:589–596
33. Costa VCI, Bueno JLO, Xavier GF (2005) Dentate gyrus-selective colchicine lesion and performance in temporal and spatial tasks. Behav Brain Res 160:286–303
34. Kesner RP, Hunsaker MR (2010) The temporal attributes of episodic memory. Behav Brain Res 215:299–309
35. Suárez-Pereira I, Canals S, Carrión AM (2015) Adult newborn neurons are involved in learning acquisition and long-term memory formation: the distinct demands on temporal neurogenesis of different cognitive tasks. Hippocampus 25:51–61
36. Counts SE, Alldred MJ, Che S, Ginsberg SD, Mufson EJ (2014) Synaptic gene dysregulation within hippocampal CA1 pyramidal neurons in mild cognitive impairment. Neuropharmacology 79:172–179
37. Bueno J, Costa VI, Xavier GF, Dima L (2006) The acquisition of a temporal task (DRL) by dentate gyrus-selective colchicine lesioned rats. Psicol Reflex Crit 19:159–165
38. Eichenbaum H, Stewart C, Morris RG (1990) Hippocampal representation in place learning. J Neurosci 10:3531–3542
39. Michalikova S, Ennaceur A, van Rensburg R, Chazot PL (2008) Emotional responses and memory performance of middle-aged CD1 mice in a 3D maze: effects of low infrared light. Neurobiol Learn Mem 89:480–488